

Effect of functional monomer on the stability and film properties of thermosetting core–shell latexes

E.P. Pedraza, M.D. Soucek*

Department of Polymer Engineering, The University of Akron, 250 S. Forge St., Akron, OH 44325-0301, USA

Received 23 February 2005; received in revised form 26 July 2005; accepted 26 August 2005

Available online 26 September 2005

Abstract

Functionalized core–shell latexes were prepared by copolymerization of butyl acrylate and methyl methacrylate with 2-hydroxyethyl methacrylate (HEMA) or methacrylic acid (MAA), which were added during the first or second stages of polymerization, respectively. The HEMA and MAA concentrations were increased while the equivalent ratio of functional groups remained constant. Colloidal stability, particle size, particle size distribution, film properties and morphology were studied as functions of functional monomer content. The upper limit functionality content was limited by the stability of the system during synthesis. A bimodal particle size distribution was observed for high concentrations of functional monomers. Increase in carboxyl and hydroxyl functionalities improved tensile strength and modulus for uncrosslinked films, and generally higher tensile strength, tensile modulus and storage modulus at high temperature were obtained after the functional latexes were crosslinked with a cycloaliphatic diepoxide.

© 2005 Elsevier Ltd. All rights reserved.

Keywords: Acrylic latexes; Functional monomer; Latex stability

1. Introduction

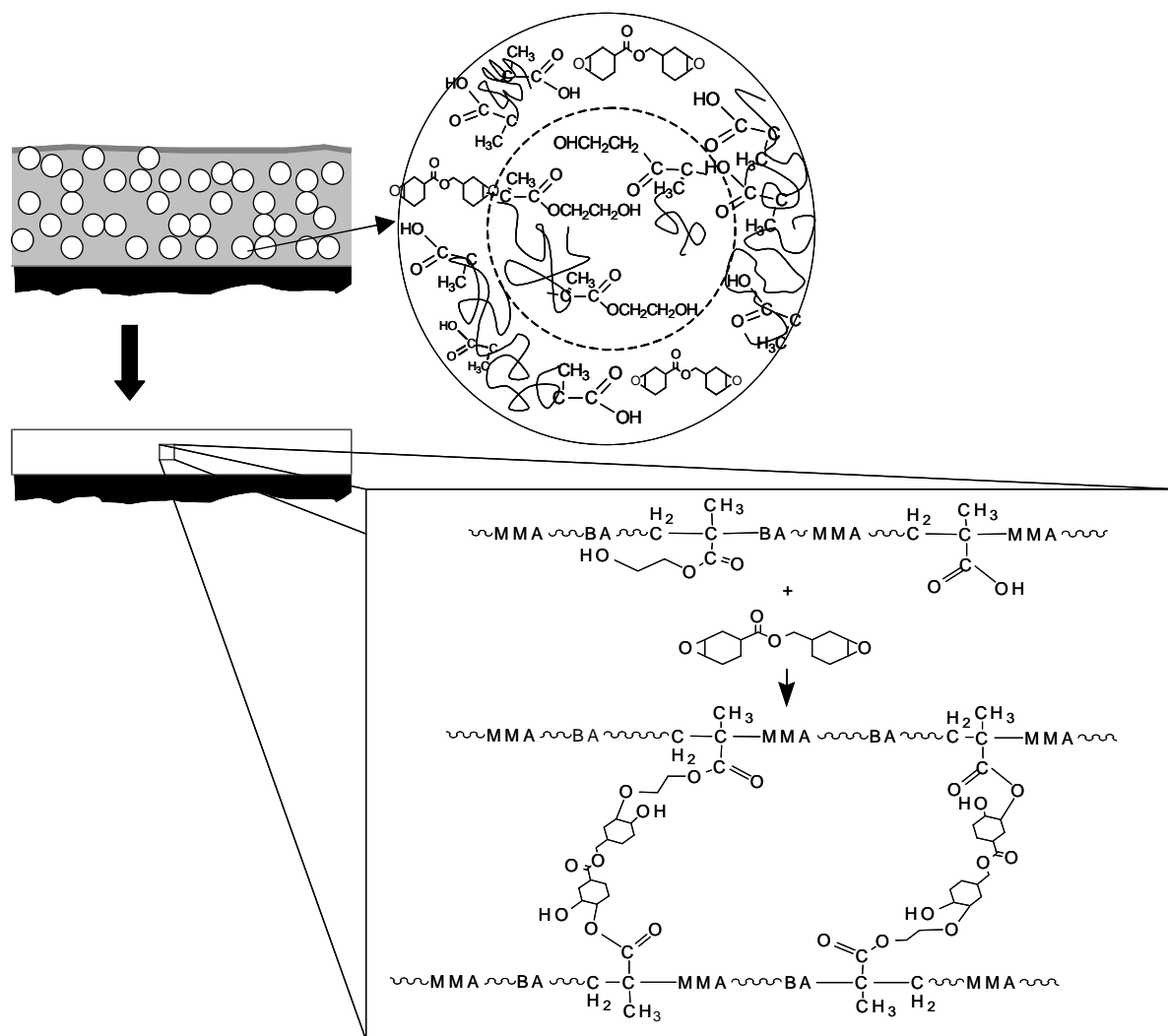
Environmental regulations have been continuously restricting the amount of volatile organic compounds (VOCs) in coatings formulations. As a consequence waterborne systems have developed, and will continue to do so as the logical choice for many applications in the coatings industry [1]. Latex based and water-reducible coatings are two major classes of waterborne coatings replacing solvent-borne applications. Latex dispersions form films at ambient temperatures by coalescence of relatively soft particles containing solid polymer. Cohesive strength development occurs during coalescence when interdiffusion of polymer chains takes place, but also by crosslinking of the polymer prior to or during film formation [2,3,5]. Generally, crosslinking is introduced into thermoplastic latex dispersions for improvement of mechanical properties and solvent resistance. Several types of thermosetting latexes have been reported in the literature in which functional monomers have been added during synthesis and then chemically crosslinked [4–14].

Previous studies in this group have shown that dispersions of latex particles containing hydroxyl-functional core and carboxylic-functional shell were successfully crosslinked with a cycloaliphatic diepoxide [15,16]. A schematic representation is shown in [Scheme 1](#). The crosslinking reactions for the system were influenced by several factors including the amount and addition mode of diepoxide, location of functional monomer, type and amount of catalyst, among others. Soucek et al. [17] investigated epoxide addition in terms of morphology and film properties obtained from the latex system. When cycloaliphatic diepoxide was added in the form of solution, increase in hardness and tensile modulus was observed possibly due to more uniform adsorption of the diepoxide on the particles surface, whereas addition of emulsified diepoxide showed lower hardness and tensile modulus. This was postulated to be a result of decreased interaction of emulsified epoxide with the latex particles [17].

In a separate study, the effect of location of hydroxyl functionality was investigated [18]. Phase inversion of the core–shell structure did not occur when hydroxyl functionality was introduced during the first stage of polymerization, indicating concentration of hydroxyl groups within the core. When hydroxyl functionality was located in the core, it promoted hardness and tensile modulus, and when it was present in the shell of the particles, higher crosslink density was observed. Distribution of functionality between both stages did

* Corresponding author. Tel.: +1 330 972 2583; fax: 1 330 258 2339.

E-mail address: msoucek@uakron.edu (M.D. Soucek).



Scheme 1. Crosslinking reaction of carboxyl and hydroxyl groups with cycloaliphatic diepoxide in a latex system.

not generally improve film properties [18]. The effect of type and concentration of catalyst was studied previously for latexes with both hydroxyl and carboxyl functional groups as sole functionality (monofunctional systems). Strong acid catalysis was required for crosslinking of hydroxyl functional latexes with cycloaliphatic diepoxide, whereas it did not necessarily improve the coating properties of latexes containing carboxyl groups [19]. It was postulated that the conjugate base of the strong acid catalyst did not undergo re-protonation under the curing conditions.

Purposeful design of these thermosetting latexes relies on the evaluation of composition variables such as addition mode of the crosslinker, type of catalyst and functionality concentration. It is desirable to have 10–20 wt% of total monomer available as functional groups to participate in crosslinking reactions; however, other properties could also be affected by increase in functionality content. Polymerization pathways, particles structure and ultimately film properties might be influenced by such change in composition. In many of previously studied formulations in the literature, functionality

varies between 2 and 8-wt% based on total monomer weight. Although such films show improved solvent resistance and enhanced mechanical properties, there is no specific information on the extent of crosslinking [4,14]. In the present study, optimization of the total amount of functional monomers was investigated, as well as consequent effects on latex and film properties. Two series of latexes were prepared with different glass transition temperatures ($T_g = 10\text{ }^\circ\text{C}$ and $T_g = -5\text{ }^\circ\text{C}$) and with increasing content of carboxyl and hydroxyl functional groups. The effects of the reacting system on colloidal stability and on particle size distribution were evaluated with varying functionality. Tensile, thermo-mechanical properties and film morphology were also evaluated.

2. Experimental

2.1. Materials

Butyl acrylate (BA), methyl methacrylate (MMA), hydroxyethyl methacrylate (HEMA), methacrylic acid (MAA),

benzyl methacrylate (BzMA), ammonium persulfate (APS), sodium bicarbonate and isopropanol were technical grade chemicals purchased from Aldrich Chemical and used as received. Dow Chemical supplied the cycloaliphatic diepoxide (UVR-6105) and surfactants Triton-200 (sodium alkylaryl polyether sulfonate) and Tergitol XJ (polyalkylene glycol monobutyl ether). Sulfoethyl methacrylate (SEM) was supplied by Hampshire/Dow Chemical. Deionized water was used in the preparation of the latexes.

2.2. Preparation of latexes

Latex dispersions were prepared by seeded semi-continuous emulsion polymerization with a monomer emulsion feed. All seeds used in the latexes synthesis were obtained from single seed latex prepared batch-wise.

2.2.1. Seed

A solution of NaHCO_3 (1.5 g) and Triton-200 (0.5 g) in water (150 g) was charged to a 500 mL flask equipped with a condenser, stirrer and a nitrogen atmosphere. After reaching 75 °C, a pre-emulsion of BA (41.68 g, 0.326 mol) and MMA (38.32 g, 0.3832 mol) with NaHCO_3 (0.1 g) and Triton-200 (3.6 g) was charged in the flask followed by addition of a 2 wt% aqueous solution of ammonium persulfate (102.2 g). Polymerization continued for 30 min at 75 °C. The same experimental apparatus for seed preparation was used for the core and shell stages.

2.2.2. Core

The seed (20 wt% of the weight of the pre-emulsion) was charged in the reactor and heated to 75 °C. A pre-emulsion of

BA, MMA and HEMA along with an initiator solution, were fed continuously for 180 min. Tables 1 and 2 list the components and amounts for each latex formulation. Contents were heated and stirred for additional 180 min to ensure monomer consumption. For Scanning Transmission Electron Microscopy, BzMA was used instead of MMA in those latexes prepared for the differential staining.

2.2.3. Shell

Following the core preparation, continuous addition of a new pre-emulsion (BA, MMA and MAA) along with fresh initiator solution proceeded over a period of 240 min. During the same time a SEM aqueous solution (5 wt%) was fed as well (this monomer was added in order to incorporate sulfonic acid groups for catalysis of crosslinking reactions after film casting). The emulsion was allowed to react for another 240 min after addition was complete. The latexes were then filtrated through a woven polymer micro-filtration mesh (20 μm mesh opening) followed by coagulum and solid contents measurements. Nomenclature is as follows: latex with formulated T_g of -5 °C and 7.4 wt% functional monomers (4.4 wt% HEMA and 3 wt% MAA) based on total content of monomer is designated as $T(-5)$ F7 (Tables 1 and 2 show other compositions). It should be noted that actual latexes glass transition temperatures are expected to differ from the values formulated, which were used for nomenclature purposes.

2.3. Latex characterization

Latexes were cleaned using an ion-exchange resin (AG-501-X8) to remove water-soluble ionic materials. Twice the weight of resin (based on latex solids) was added to dilute latexes

Table 1
Composition for core and shell compositions for latexes with different percentages of functional monomer (based on total monomer) and designed $T_g = 10$ °C

| Component | $T(10)$ F7 ^a (7.5 wt%) ^b | | $T(10)$ F15 ^a (15 wt%) ^b | | $T(10)$ F17 ^a (17.5 wt%) ^b | |
|--------------------------------|--|-----------------------|--|---------------------|--|----------------------|
| | Core weight (g) | Shell weight (g) | Core weight (g) | Shell weight (g) | Core weight (g) | Shell weight (g) |
| BA | 35.75 | 37.89 | 35.32 | 39.66 | 35.18 | 40.23 |
| MMA | 37.10 | 37.38 | 30.28 | 30.74 | 27.98 | 28.62 |
| HEMA | 7.14 (0.055 equiv) | – | 14.4 (0.11 equiv) | – | 16.9 (0.13 equiv) | – |
| MAA | – | 4.73 (0.055 equiv) | – | 9.6 (0.11 equiv) | – | 11.2 (0.13 equiv) |
| SEM ^c | – | 0.57 | – | 0.57 | – | 0.57 |
| NaHCO_3 | 0.1 | 0.1 | 0.1 | 0.1 | 0.1 | 0.1 |
| Triton-200 | 3.6 | 3.6 | 3.6 | 3.6 | 3.6 | 3.6 |
| Tergitol-XJ | 0.4 | 0.4 | 0.4 | 0.4 | 0.4 | 0.4 |
| Water | 80.0 | 80.0 | 80.0 | 80.0 | 80.0 | 80.0 |
| Diepoxide ^d | – | 13.86 | – | 27.72 | – | 32.76 |
| Isopropanol | – | 13.86 | – | 27.72 | – | 32.76 |
| Coagulum in grams ^e | 0.05 | – | 1.09 | – | 1.91 | – |
| Solid content (%) | 38.5 | – | 37.3 | – | 36.7 | – |

^a T stands for formulated T_g in degrees centigrade (°C); F stands for functionality; the last number shows total functionality percentage based on total monomer content.

^b Total functional monomers weight percentage based on total monomer content.

^c SEM stands for sulfoethyl methacrylate.

^d Crosslinker was added after latex synthesis.

^e Coagulum formed during reaction.

Table 2
Composition for core and shell compositions for latexes with different percentages of functional monomer (based on total monomer) and designed $T_g = -5^\circ\text{C}$

| Component | $T(-5) F7^a$ (7.5 wt%) ^b | | $T(-5) F15^a$ (15 wt%) | | $T(-5) F21^a$ (21 wt%) | |
|--------------------------------|-------------------------------------|------------------|------------------------|------------------|------------------------|------------------|
| | Core weight (g) | Shell weight (g) | Core weight (g) | Shell weight (g) | Core weight (g) | Shell weight (g) |
| BA | 44.14 | 46.29 | 43.71 | 48.06 | 40.48 | 46.53 |
| MMA | 28.71 | 28.98 | 21.89 | 22.34 | 19.52 | 20.09 |
| HEMA | 7.14 | – | 14.4 | – | 20.0 | – |
| | (0.055 equiv) | – | (0.11 equiv) | – | (0.154 equiv) | – |
| MAA | – | 4.73 | – | 9.6 | – | 11.2 |
| | – | (0.055 equiv) | – | (0.11 equiv) | – | (0.154 equiv) |
| SEM ^c | – | 0.57 | – | 0.57 | – | 0.57 |
| NaHCO ₃ | 0.1 | 0.1 | 0.1 | 0.1 | 0.1 | 0.1 |
| Triton-200 | 3.6 | 3.6 | 3.6 | 3.6 | 3.6 | 3.6 |
| Tergitol-XJ | 0.4 | 0.4 | 0.4 | 0.4 | 0.4 | 0.4 |
| Water | 80.0 | 80.0 | 80.0 | 80.0 | 80.0 | 80.0 |
| Diepoxide ^d | – | 13.86 | – | 27.72 | – | 38.81 |
| Isopropanol | – | 13.86 | – | 27.72 | – | 38.81 |
| Coagulum in grams ^e | 0.21 | – | 1.63 | – | 3.72 | – |
| Solid content (%) | 39.3 | – | 37.4 | – | 36.8 | – |

^a T stands for formulated T_g in degrees centigrade ($^\circ\text{C}$); F stands for functionality; the last number shows total functionality percentage based on total monomer content.

^b Total functional monomers weight percentage based on total monomer content.

^c SEM stands for 2-sulfoethyl methacrylate.

^d Crosslinker was added after latex synthesis.

^e Coagulum formed during reaction.

(10% solids); the mixture was stirred at ambient temperature for 2 h, and then vacuum filtered. The process was repeated twice. Particle morphology was examined by STEM using a FEI Tecnai 12 Microscope. Particle sizes and particle size distributions were measured by dynamic light scattering using a PSS NICOMP (Santa Barbara, CA) equipped with a He–Ne laser operating at 652 nm and a triple detector. Measurements were carried out at 23 $^\circ\text{C}$ and at a fixed angle of 90 $^\circ$ on very diluted emulsions (<0.1 vol%). Molecular weight was determined by gel permeation chromatography (GPC) using high-resolution Waters columns with THF at 1 mL/min. A triple detector was used comprising a Viscotek viscometer, a Waters differential refractometer and a Wyatt Dawn EOS light scattering detector at 90 $^\circ$. Particle morphology was evaluated for latexes containing benzyl methacrylate. This monomer was introduced during the first stage of the polymerization to differentiate between the core and shell via RuO₄ staining. For STEM sample preparation, a drop of clean and very dilute latex (0.5 wt%) was placed onto a carbon coated copper grid and set to dry for 2 h at ambient temperature. Samples on grids were exposed to RuO₄ vapors for 15 min and dried under ambient conditions for 24 h prior to imaging.

2.4. Film formation and characterization

Cycloaliphatic diepoxide was dissolved in isopropanol (50 wt%). Latexes were neutralized with ammonia at ambient temperature to pH=7. Stoichiometric amounts of the diepoxide solution were added, and mixtures were stirred for 15 min (Table 1). Then, latexes were cast on glass and aluminum substrates using a draw down bar #8 (8 mil for wet

thickness). The final thickness of the samples was between 40 and 60 μm . Dry films were obtained either after 48 h of drying at ambient temperature or after drying 2 h at ambient temperature followed by heating at 170 $^\circ\text{C}$ for 1 h. Films cast on glass were removed with a razor blade and cut (80 \times 16 mm or 25 \times 5 mm) for tensile testing on an Instron Universal Electromechanical Tester 5567 and dynamic mechanical thermal analysis using a Rheometrics Scientific analyzer. Tensile testing was performed with a load cell of 100 N and a crosshead speed of 20 mm/min. More than 10 specimens were tested and those with closest values were selected to obtain average values (selection criteria according to ASTM standard D2370-98). Dynamic mechanical thermal analyses were carried-out with a constant temperature ramp (3 $^\circ\text{C}/\text{min}$), a fixed oscillating frequency (1 Hz) and a controlled strain (0.5%). Films cast on aluminum were used for coatings testing such as pencil hardness (D 3363-00), impact resistance (ASTM G 14), flexibility (conical mandrel testing ASTM D 522) and MEK double rubs (ASTM D 4752-98). Latexes were spin-coated onto pre-treated silica wafers and examined for dry film morphology in a Multimode Scanning Probe Microscope (Digital Instruments) set to tapping mode.

3. Results

The primary objective of this study was to investigate the effect of functional monomers concentration and concomitant equimolar addition of crosslinker on stability and film properties of crosslinkable latexes. Reactions of attached carboxyl and hydroxyl functionalities with cycloaliphatic diepoxides are influenced by the concentration of reacting

groups, by mobility of the polymer segments and by acid catalysis during crosslinking. Increasing functional monomer concentration is not only expected to affect crosslinking reactions, but it can also introduce changes during synthesis and to latex properties [4]. Moreover, it is anticipated that increasing hydroxyl functionality in the core and carboxyl functionality in the shell would bring dissimilar chemical and physical properties. The relationship between monomer composition (including functional monomers) and glass transition temperature was taken into account in designing the latexes. Consequently, two series of latexes were prepared with different T_g and increasing equimolar content of HEMA and MAA varying from 7.4 to 21 wt%. Glass transition temperatures of -5 and 10°C were calculated by the Fox equation [20].

The double functionality approach was preferred due to superior film properties obtained through crosslinking, compared to mono-functional systems [15]. The choice of placement of functional groups was based on two reasons. First, previous studies in this group showed that HEMA-containing copolymer located in the core of particles did not cause core-shell inversion of the latex particles under the polymerization conditions used [18]. Second, when carboxylic acid groups were added during the core stage and hydroxyl groups during the shell stage, latexes were unstable [16]. As a result, the preferred morphology in terms of latex stability and films performance consisted of hydroxyl groups located in the core and carboxylic acid groups placed in the shell.

The addition of diepoxide to the latex was performed in the form of a solution, due to the very low solubility of the epoxide in water. As investigated previously [17], addition of the crosslinker as a solution resulted in overall best films properties. This result was attributed to increased adsorption on particles surface. Atom Force Microscopy (AFM) images supported such consideration. Additionally, in a previous study [18], successful crosslinking was obtained for latexes containing only hydroxyl functionality incorporated during the core stage. The extent of crosslinking was lower than in the case of hydroxyl groups located in the shell, but crosslinking was achieved. Furthermore, films properties were enhanced compared to uncrosslinked systems. Such results suggested that a small portion of epoxide migrates within the polymer during film formation. It is then expected that a portion of diepoxide, located in the proximity of particles in the emulsion, are driven towards the surface of particles by its low water solubility. It is also expected that a small portion of epoxide might continue to move inside the particle. Consequently, addition of epoxide as a solution in isopropanol was considered highly beneficial in terms of film property development.

Total maxima of 17.5 and 21 wt% functional monomers were successfully incorporated in the formulation of series $T(10)$ and $T(-5)$, respectively. The upper functionality limit in these latexes was determined by the maximum HEMA concentration introduced during the first stage of polymerization without causing instability of the emulsion. For series $T(10)$, adding more than 10 wt% HEMA in the co-monomer feed led to disruption of colloidal stability during the first stage

of polymerization. However, for series $T(-5)$, it was possible to add up to 12.5 wt% HEMA without emulsion break-up. Coagulum measured after polymerization increased upon addition of larger functionality amounts in the co-monomer feed, which indicated some degree of instability in the system during reaction.

3.1. Latex properties

During the synthesis process or afterward it is possible that the desired core-shell structure of the particles might have not been obtained, since particle morphology is highly affected not only by thermodynamic parameters but also by kinetic factors [21–28]. In this particular case, it was anticipated that increments in functional monomer concentration might have interfered with the equilibrium morphology of the system. For this reason, the morphology of the latexes was evaluated by STEM. During synthesis of some of the latexes, a fraction of non-functional monomer mixture was replaced by benzyl methacrylate in the core polymerization stage. Benzyl methacrylate (BzMA) was introduced to achieve facile staining with RuO_4 and was preferred over styrene because it is less chemically dissimilar to the acrylic system. An image of latex particles with $T_g = -5^\circ\text{C}$ and 15 wt% functional monomers is shown in Fig. 1. The first stage polymer seems to be located at the centre of the particle as evidenced by dark domains. This suggests that the core-shell structure was not disrupted by increased fractions of HEMA and MAA during polymerization.

Together with changes in particle structure, other latex properties might have been altered upon increasing functionality content. As general latex characterization, molecular weight and particle size were evaluated. For molecular weight measurements, dry films were immersed in THF for several days; still, complete dissolution was not achieved. A few minutes under sonication dissolved the remaining gel. Same sonication time was allowed for all samples; however, the sample with 0 wt% functional monomers retained a small

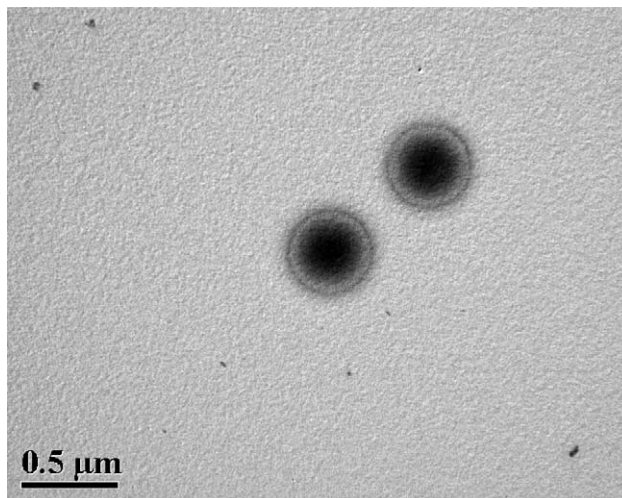


Fig. 1. STEM image of core-shell latex with 9 wt% HEMA and 6 wt% MAA.

Table 3
Molecular weight and particle size for latexes with designed $T_g = -5^\circ\text{C}$

| Name | Functionality (wt% total monomer) | Molecular weight (g/mol) M_w | Particle size (nm) | |
|-------------|-----------------------------------|--------------------------------|----------------------------|---------------------------|
| | | | Peak 1/standard deviation | Peak 2/standard deviation |
| $T(-5)$ F0 | 0 | 1,328,300 | 364.0/57.9 | – |
| $T(-5)$ F7 | 7.4 | 835,900 | 348.0/55.0 | – |
| $T(-5)$ F15 | 15.0 | 562,400 | 345.6/12.1 | – |
| $T(-5)$ F21 | 21.0 | 440,400 | 215.8 (51.7%) ^a | 704.0 (48.3%) |

^a Standard deviation not available. Proportion of particles for each size reported as percentage.

amount of gel that plugged the filter prior to injection. For such reason these values are considered as relative in this case. Molecular weight and particle size of latexes from series $T(-5)$ are presented in Table 3. Weight-average molecular weight values showed a decreasing trend as HEMA and MAA concentrations increased. Latexes with up to 15 wt% functionality showed similar particle size (around 350 nm). In the case of maximum functionality content (21 wt%) two populations of particles with different sizes were observed.

3.2. Film properties

Films were evaluated for typical coatings tests, tensile properties and dynamic mechanical properties. Table 4 presents coatings properties for films obtained from mixtures of latexes series $T(10)$ and cycloaliphatic epoxide solution (films were cast and dried under ambient conditions for 2 h followed by heating at 170°C for 1 h). As seen from the table, typical coating tests such as pencil hardness, impact resistance, conical mandrel flexibility and MEK double rubs exhibited only small variations for these films. For instance, all films showed conical mandrel flexibilities superior to 32% and MEK double rubs above 200. For this reason, tensile testing and dynamic mechanical analysis were preferred for evaluation and contrast of film properties.

Tensile testing is a very useful tool for evaluation of mechanical properties in free films. Tensile properties of latexes from series $T(-5)$ ($T_g = -5^\circ\text{C}$) are summarized in Figs. 2 and 3. Fig. 2 clearly shows that tensile strength and

tensile modulus values uniformly increased upon introduction of increasing levels of HEMA and MAA for films cast from latexes without crosslinker. Conversely, elongation-at-break was severely reduced as functionality content was increasing in the latex formulation. When crosslinker was introduced, tensile strength and modulus were improved significantly as expected with respect to films without crosslinker especially at very high functionality content. Elongation-at-break reduction was not as severe for crosslinked films as compared to films without crosslinker, for which elongation decreased from approximately 500 to 100% or lower.

Dynamic mechanical thermal analysis was performed on films cast from latex series $T(-5)$ ($T_g = -5^\circ\text{C}$). The storage modulus E' at the rubbery equilibrium region above T_g is related to the crosslink density by the classical expression [29,30]

$$\nu_e = \frac{E'}{3RT}$$

where ν_e is the crosslink density expressed as moles of elastically effective network chains per cubic meter of sample. E' is the storage modulus at the equilibrium plateau, R is the gas constant ($8.3145 \text{ Pa m}^3/\text{mol K}$) and T is the temperature in Kelvin. Figs. 4 and 5 show the temperature dependence of storage modulus E' and loss tangent ($\tan \delta$) for films without crosslinker dried at ambient temperature. It was observed that as concentration of functional monomers increases in the films, there was progressive broadening in the transition region detected on both, storage modulus E' and $\tan \delta$ peak signals. In the same way, the maximum value for $\tan \delta$ decreased and the temperature at that point shifted toward higher temperatures as functionality content was increased. Figs. 6 and 7 show storage modulus E' and $\tan \delta$ responses for the same type of films (without crosslinker) dried at ambient temperature for 2 h and heated at 170°C for 1 h. Heating did not seem to cause much effect on the broadening of the transition region observed for films just dried at room temperature. However, the storage modulus signal reaches a plateau above the glass transition temperature for latex $T(-5)$ F21, which holds the maximum functional monomer content possible for this series.

Storage modulus and loss tangent plots for films cast from mixtures of latexes $T(-5)$ with cycloaliphatic epoxide solution are shown in Figs. 8 and 9. As similarly observed for uncrosslinked films, the relatively sharp drop in storage modulus characteristic of the glass transition region was broader as functional monomers concentration was incremented. It was also observed that upon increments in the functionality content the one $\tan \delta$ peak originally detected developed into two broad and indistinct peaks. Table 5 presents a summary of the characteristic dynamic properties obtained for these films. Glass transition temperatures, storage moduli at the rubbery plateau and crosslink densities were observed to increase as HEMA and MAA contents were augmented.

Morphology of films obtained through AFM imaging is shown in Fig. 10. Latexes $T(-5)$ with 0 and 7.4 wt% functional monomers (Fig. 10(a) and (b), respectively) showed similar average particle size. However, Fig. 10(c) evidenced

Table 4
Coatings testing for latexes with designed T_g of 10°C and total functionality from 7.4 to 17.5 wt% (series $T(10)$) crosslinked with cycloaliphatic diepoxide

| Test | $T(10)$ F7 | $T(10)$ F15 | $T(10)$ F17 |
|------------------------------------|------------|-------------|-------------|
| Pencil hardness | 2H | 4H | 3H |
| Conical mandrel (% elongation) | > 32 | > 32 | > 32 |
| Impact resistance (direct/inverse) | > 40/> 40 | 30/> 40 | > 40/> 40 |
| MEK double rubs | > 200 | > 200 | > 200 |

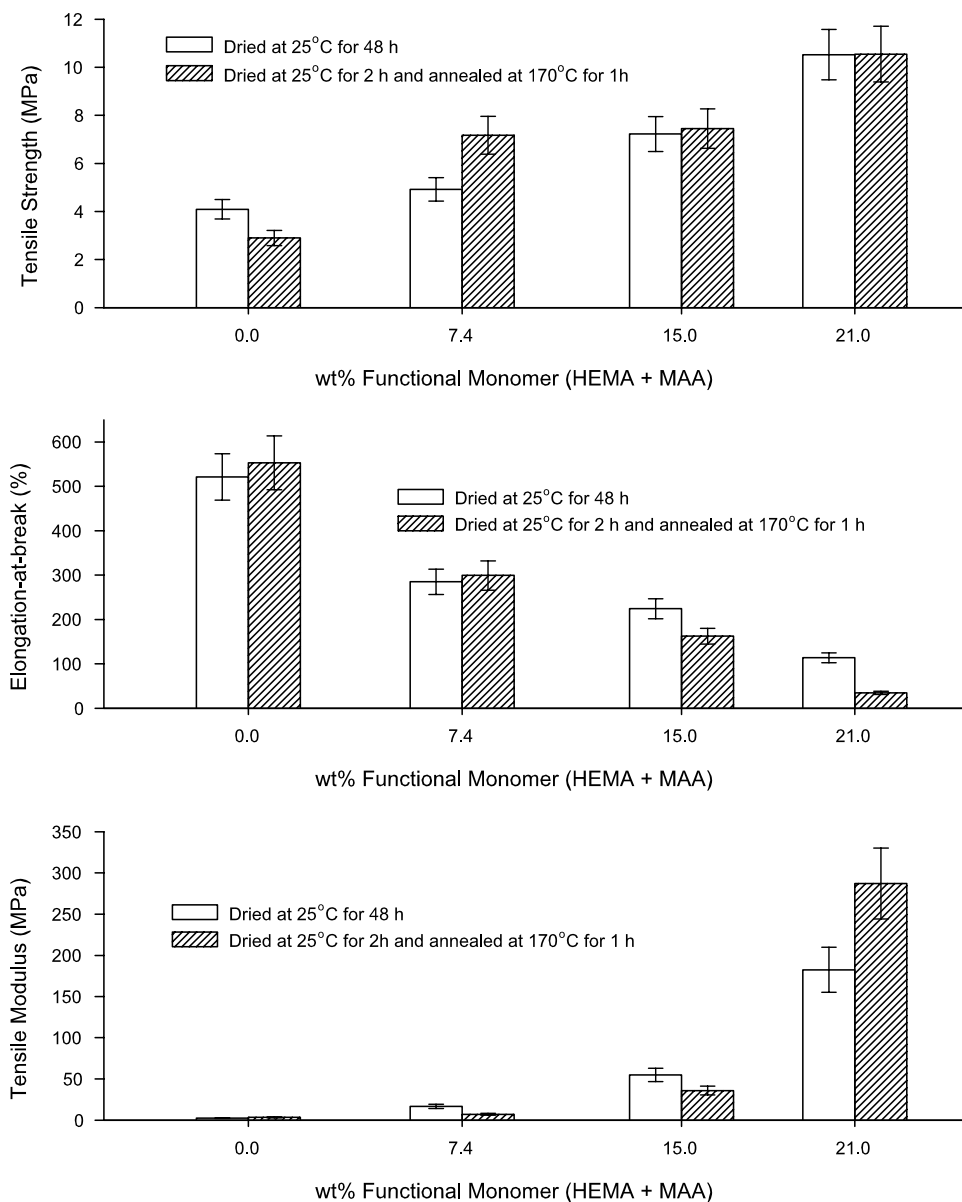


Fig. 2. Tensile properties of films from latex with designed $T_g = -5$ °C.

two different populations of particles: one of small particles and one of larger particles. Such observation appeared in agreement with particle size measurements. Images from films dried at 25 °C during 2 h and heated for 1 h at 170 °C showed reduced presence of discrete particles, although incomplete coalescence was observed.

4. Discussion

Several reasons motivated the study of functionality content in thermosetting acrylic core-shell latexes. Initially, optimization of the upper limit functionality concentration was basic to achieve maximum strengthening in these types of films. Additionally, it was anticipated that the polymerization process and latex characteristics could also be affected by incorporation of increasing content of functional monomers. For instance, the

pathway of polymerization is often dependent on the type of monomers involved, affecting molecular weight and particle size. Consequently, it was necessary to evaluate the effect of increasing co-monomer functionality content on latex stability and films properties.

The larger fraction of HEMA (and total HEMA and MAA content) successfully incorporated in series $T(-5)$ compared to series $T(10)$ and its effect on latexes particle populations can be explained by monomer solubility and copolymerization effects. It should be considered that as the fraction of HEMA in the monomer mixture was increased, the concentration of this monomer in the aqueous phase was higher due to its increased water solubility compared to MMA or BA (solubilities in water: 81, 1.6 and 0.2 g/100 mL, respectively) [31–33]. Additionally, taking into account reactivities for the three monomers in Table 6 [34], it could be expected that HEMA

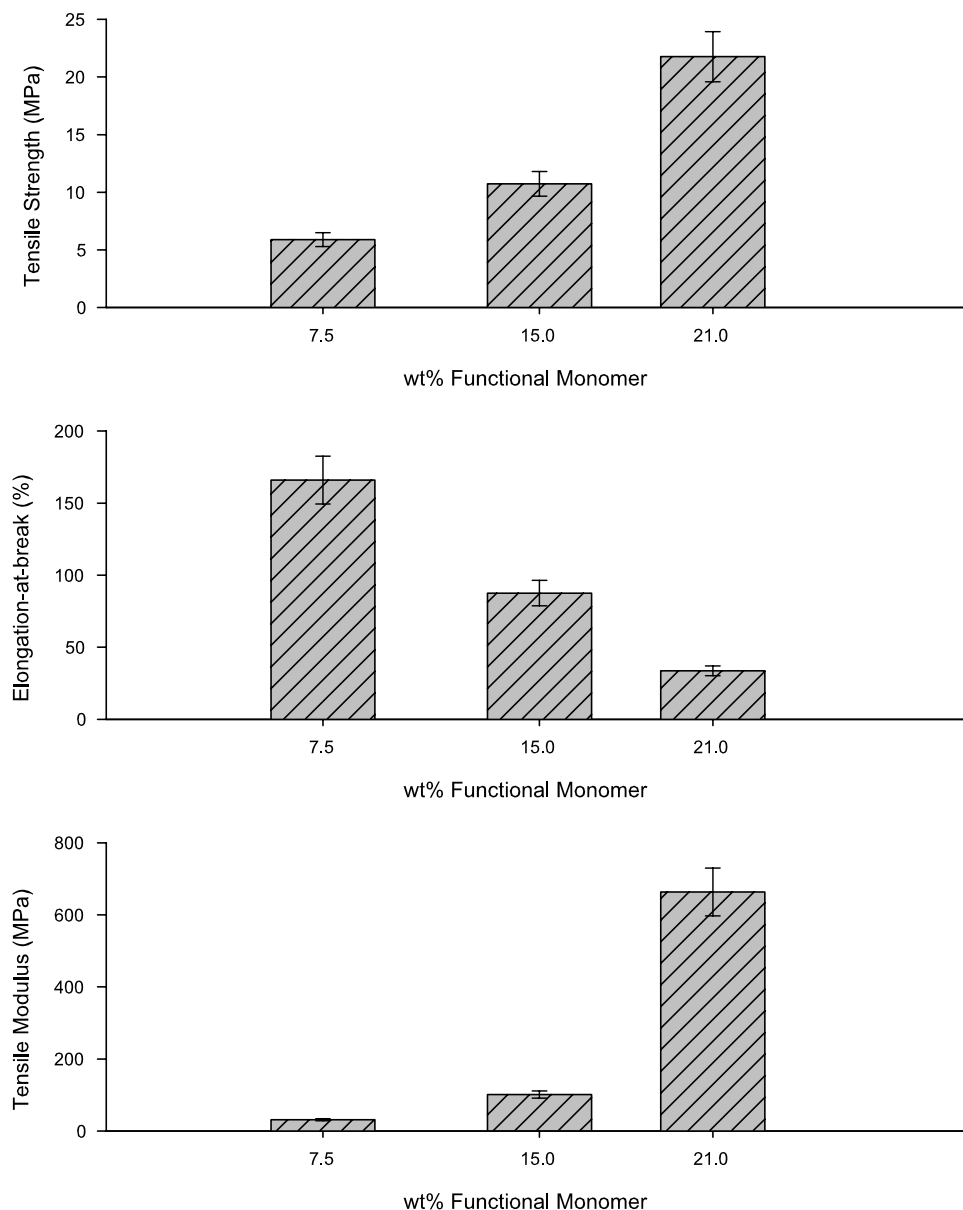


Fig. 3. Tensile properties of crosslinked films from latex series $T(-5)$.

molecules were more prone to react with other HEMA molecules than with MMA and BA molecules present in the system.

It is commonly known that the initiation process during most emulsion polymerizations usually occurs in the aqueous phase with formation of hydrophilic oligomeric radicals. Upon growth, these oligomeric radicals would not enter monomer-swollen micelles until reaching a critical entry chain length for which a hydrophilic-hydrophobic balance would be achieved. These oligomeric radicals might or might not become soluble; if not soluble, such oligomers precipitate out of solution and are stabilized by adsorption of surfactant, forming new particles (homogeneous nucleation) [35]. Such scenario is represented in Scheme 2. In these systems, as BA/MMA ratio was larger (1.13 in series $T(10)$ to 1.87 in series $T(-5)$ on average), formation of oligomeric radicals was influenced by

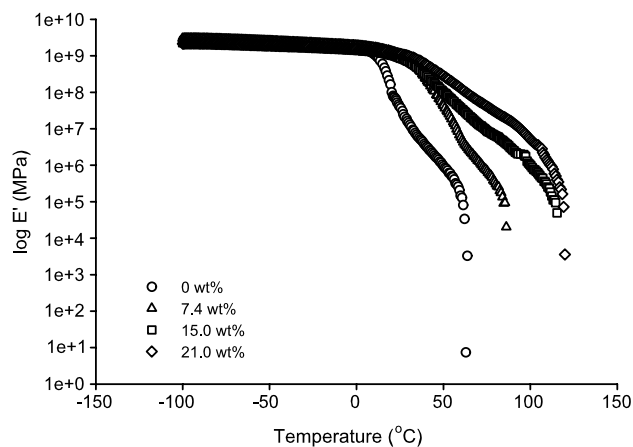


Fig. 4. Storage modulus of films from latexes with designed $T_g = -5$ °C dried at 25 °C for 48 h (no crosslinker added).

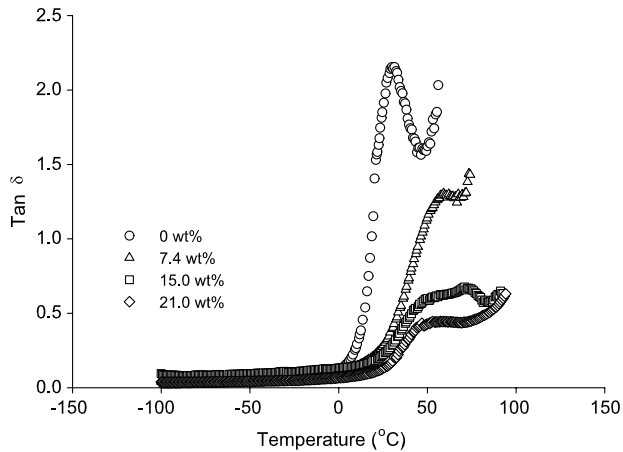


Fig. 5. $\tan \delta$ of films from latexes with designed $T_g = -5^\circ\text{C}$ dried at 25°C for 48 h (no crosslinker added).

the presence of the less water-soluble BA, possibly by changing the solubility of oligomeric species at the critical chain length at which such oligomers would either precipitate out of solution or enter the organic phase.

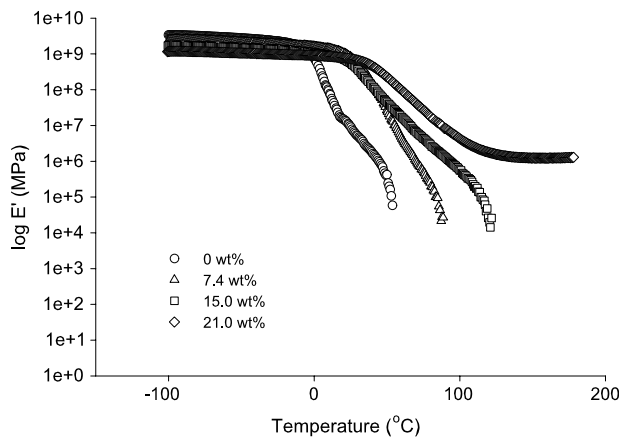


Fig. 6. Storage modulus of films from latexes with designed $T_g = -5^\circ\text{C}$ dried at 25°C for 2 h and heated at 170°C for 1 h (no crosslinker added).

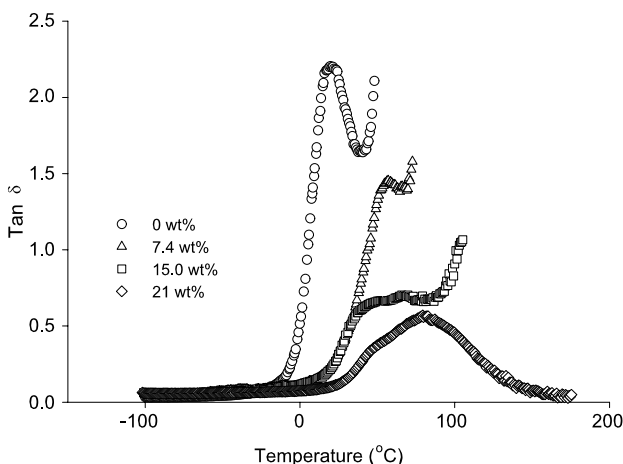


Fig. 7. $\tan \delta$ of films from latexes with designed $T_g = -5^\circ\text{C}$ dried at 25°C for 2 h and heated at 170°C for 1 h (no crosslinker added).

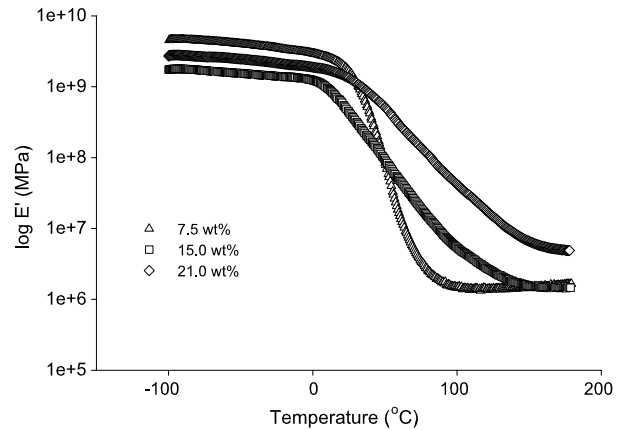


Fig. 8. Storage modulus of crosslinked films from latexes with designed $T_g = -5^\circ\text{C}$.

Poehlein [36] studied the emulsion polymerization of styrene in the presence of water-soluble co-monomers and found that for styrene-methacrylic acid systems, the entry size and composition of oligomeric species changed as the ratio between monomers varied. As more MAA was used, a higher MAA/Styrene ratio was observed in the oligomers. Moreover, the molecular weight of the species increased [36]. Correspondingly, if increasing concentration of HEMA molecules in the aqueous phase were determinant in the stability of the system during polymerization, it would be most reasonable to think that less-soluble oligomers led to formation of new particles. This hypothesis would explain the two particle sizes observed for the latex containing the maximum amount of functional monomers (21 wt%). In fact, generation of particles during polymerization of monomers with high water solubility such as vinyl acetate (solubility 2.5 g/100 mL) has been shown to occur via precipitation of aqueous oligomeric radicals [37]. Similarly, previous studies on polymerization of methyl methacrylate in aqueous solution have shown particle formation during reaction [38].

In the case of the latex with two particle populations that was observed in this study (at 12.5 wt%), the presence of

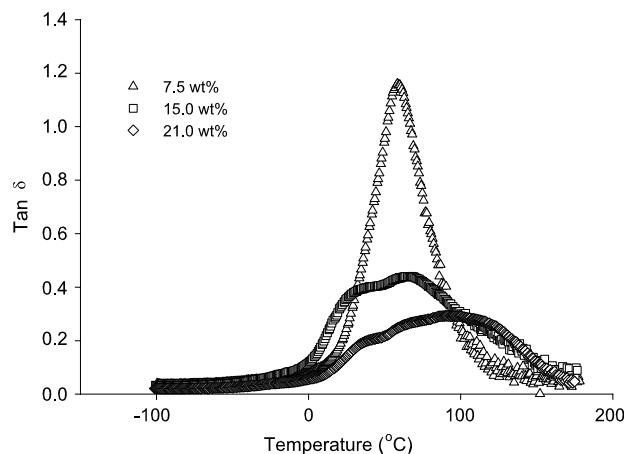


Fig. 9. $\tan \delta$ of crosslinked films from latexes with designed $T_g = -5^\circ\text{C}$.

Table 5
Dynamic properties and crosslink density for crosslinked films from latexes with designed $T_g = -5^\circ\text{C}$

| | T_g ($^\circ\text{C}$) | Max. $\tan \delta$ | Peak width ($^\circ\text{C}$) | E' (MPa) | ν_e (mol/m ³) |
|-------------|----------------------------|--------------------|---------------------------------|--------------|-------------------------------|
| $T(-5)$ F7 | 59.2 | 1.16455 | 44.99 | $1.4 + 106$ | 146.8 |
| $T(-5)$ F15 | 69.7 | 0.44994 | 122.32 | $2.15 + 106$ | 211.7 |
| $T(-5)$ F21 | 93.7 | 0.30816 | 128.19 | $8.94 + 106$ | 859.8 |

water-soluble HEMA molecules in the aqueous phase and its prominent reactivity probably boosted homogeneous nucleation, which would not be very significant compared to micellar nucleation in the polymerization of water-insoluble monomers. When concentration of water-soluble HEMA was increased to this level, more HEMA-rich oligomeric radicals could have led to secondary nucleation of particles. Above 12.5 wt% HEMA content, too many oligomeric radicals were probably generated, and stability of the colloidal system was compromised.

Stress–strain analyses as well as dynamic mechanical analysis were performed on films obtained from latexes with increasing functionality and crosslinker content. Upon addition of crosslinker, films showed pronounced enhancement in

tensile strength and tensile modulus as HEMA and MAA concentrations were increased. This improvement is evidence of cohesive strength development within films achieved through crosslinking. Flexibility of the films was reduced, as measured by elongation at the moment of breakage. Such reduction in elongation was expected due to higher concentration of joint sites between polymer chains, which restrict movement upon stretching. More interestingly, tensile strength and tensile modulus for films without crosslinker improved uniformly upon increasing content of HEMA and MAA. Such behavior might be the result of increasing interaction forces between polar groups in polymer chains (i.e. hydrogen bonding among carboxyl and hydroxyl groups).

The dynamic mechanical analysis of films with increasing functionality concentrations showed two major trends. One corresponded to broadening of the transition region and the other represented the shift of the maximum $\tan \delta$ value toward lower numbers and higher temperatures. Hidalgo and co-workers found a similar broadening for polystyrene/poly(butyl acrylate-methacrylic acid) core–shell latexes with increasing content of MAA (MAA fractions were smaller than in this study) [39]. It was considered as a result of composition drift during copolymerization due to difference in reactivity ratios that produced chains with wide composition distribution and wide range of transition temperatures. This may also be the case for latexes $T(-5)$. Through the transition region, the storage modulus values were larger as functional monomer content was increased. The role of hydrogen bonding discussed previously as being the reason for increased strength in uncrosslinked films, may as well explain the increase in storage modulus and the rubbery plateau observed for the sample containing 21 wt% functionality. Additionally to the broadening of the transition region, it was observed that a secondary $\tan \delta$ peak developed upon increments in functionality fraction. Broad transitions have been often related to samples that undergo partial phase separation during crosslinking. Furthermore, the presence of two indistinct and broad peaks in the $\tan \delta$ signal, as observed in this case, may indicate phase separation (of the core–shell structure) with substantial mixing at the boundaries between domains [29].

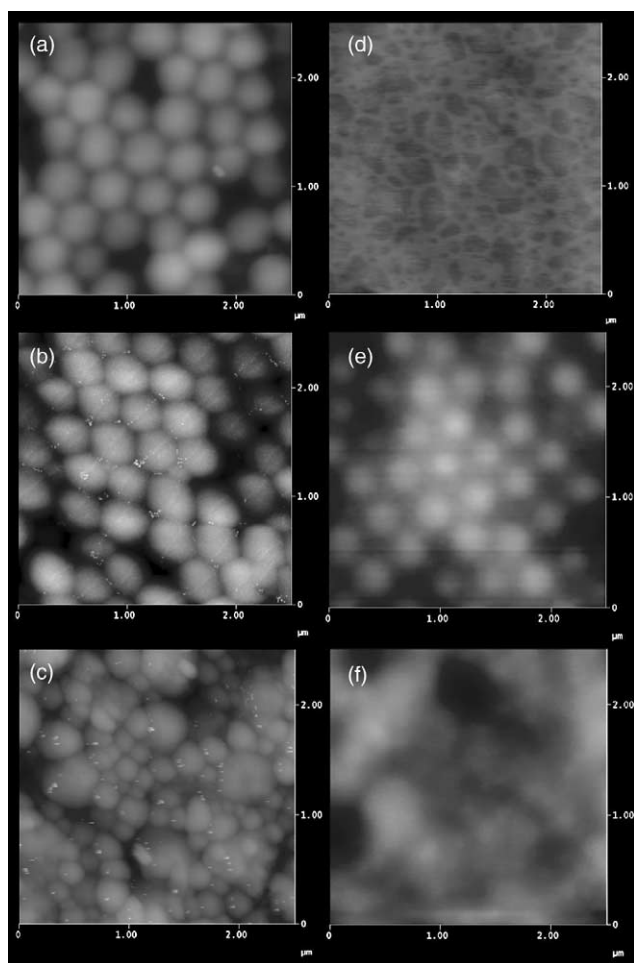
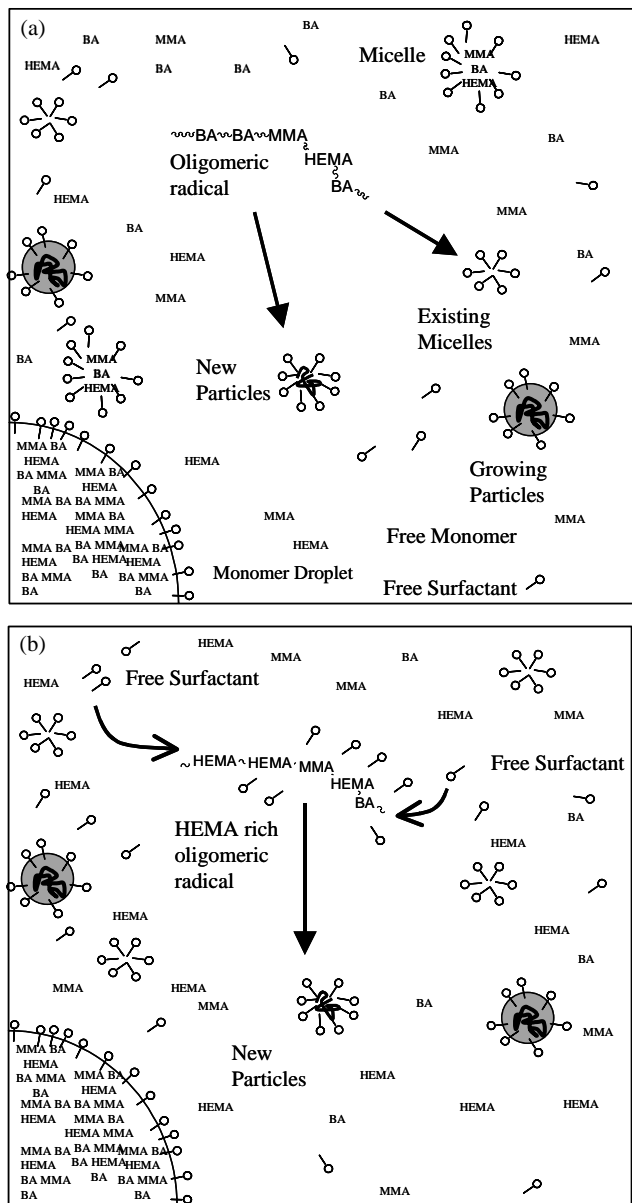


Fig. 10. Tapping mode AFM images (height mode) for latexes with 0, 7.4 and 21 wt% functional monomers dried at 25°C for 48 h ((a)–(c), respectively). Same latexes heated at 170°C for 1 h ((d)–(f)).

Table 6
Reactivity ratios for pairs of HEMA, MMA and BA (from Ref. [34])

| M1 | M2 | r_1 | r_2 |
|-----|------|-------|-------|
| BA | MMA | 0.13 | 0.92 |
| BA | HEMA | 0.09 | 4.75 |
| MMA | HEMA | 0.192 | 0.81 |



Scheme 2. Representation of particle nucleation dependence on oligomeric radicals solubility. (a) Water solubility of oligomeric radicals determine the stability of the system. (b) Homogeneous nucleation may occur for many of the HEMA-rich oligomeric radicals.

Images from films dried at 25 °C during 2 h and heated for 1 h at 170 °C showed incomplete coalescence, since discrete particles were still visible with some degree of deformation. Polymer interdiffusion in systems with particles containing hydrophilic shells such as this type of latexes has been previously studied. It was shown that interdiffusion was retarded at temperatures below the T_g of the polymer located in the shell [40]. It is proposed that inter-particle crosslinking may be the major factor favoring cohesive strength within these films. Such crosslinking position accounted for large increases in tensile strength, tensile modulus and thermo-mechanical properties even though interdiffusion across particle boundaries was not complete when crosslinking reactions occurred.

The implications of increasing functionality, in particular combinations of hydroxyl and carboxyl groups on latex dispersions are complex. Before the consummate intention of crosslinking, controlled preparation and stability of the system may be compromised. Secondary nucleation, if controlled, would have certain advantages with respect to enhanced coalescence and separation of functional groups on a mesoscale; thus, this is an area of further study at this point. Optimum functionality content of a latex system that was stable corresponded to 9 wt% hydroxyl functional monomer in the core and 6 wt% carboxyl functional monomer in the shell, for a total functionality of 15 wt% based on total monomer.

5. Conclusions

Latexes with high functionality content (HEMA and MAA monomers) were synthesized by a two-stage emulsion polymerization. The maximum possible content of functional monomers incorporated was determined by colloidal stability of the system. When large fractions of functional monomers were copolymerized, presumed secondary nucleation occurred during the first stage of polymerization. Pronounced increment in films strength observed for uncrosslinked films was explained as a consequence of increased interactions between functional groups within the films.

References

- [1] Wicks ZW, Jones FN, Pappas SP. Organic coatings: science and technology. New York: Wiley; 1998 [chapter 8].
- [2] Winnik MA. The formation and properties of latex films. In: Lovell PA, El-Aasser MS, editors. Emulsion polymerization and emulsion polymers. New York: Wiley; 1997. p. 467–518.
- [3] Daniels ES, Klein A. Prog Org Coat 1991;19:359–78.
- [4] Bufkin BG, Grawe JR. J Coat Technol 1978;50(641):41–55.
- [5] Taylor JW, Winnik MA. J Coat Technol Res 2004;1(3):163–90.
- [6] Bashleben CP, Shay GD, Smith AD. US Patent No. 4529767; 1985.
- [7] Huang Y, Jones FN. Prog Org Coat 1996;28:133–41.
- [8] Taylor JW, Basset DR. The application of carbodiimide chemistry to coatings. In: Glass LE, editor. Technology for waterborne coatings. Washington, DC: American Chemical Society; 1997. p. 137–63.
- [9] Pollano G. Polym Mater Sci Eng 1997;77:383–4.
- [10] Chen MJ, Osterholtz FD, Chaves A, Ramdatt PE. J Coat Technol 1997; 69(875):49–55.
- [11] Inaba Y, Daniels ES, El-Aasser MS. J Coat Technol 1994;66(833):63–74.
- [12] Geurink PJA, van Daden L, van der Ven LGJ, Lamping RR. Prog Org Coat 1996;27:73–8.
- [13] Nabuurs T, Baijards RA, German AL. Prog Org Coat 1996;27:163–72.
- [14] Wu S, Soucek MD. Polymer 2000;41:2017–28.
- [15] Teng G, Soucek MD. Polymer 2001;42:2849–62.
- [16] Soucek MD, Teng G, Wu S. J Coat Technol 2001;73(921):117–25.
- [17] Teng G, Soucek MD, Yang XF, Tallman DE. J Appl Polym Sci 2003;88: 245–57.
- [18] Teng G, Soucek MD. J Polym Sci, Part A: Polym Chem 2002;40: 4256–65.
- [19] Wu S, Jorgensen JD, Skaja AD, Williams JP, Soucek MD. Prog Org Coat 1999;36:21–33.
- [20] Fox T. Bull Am Phys Soc 1956;1:123.
- [21] Sundberg DC, Casassa AP, Pantazopoulos J, Muscato MR, Kronberg B, Berg B. J Appl Polym Sci 1990;41:1425–42.
- [22] Chen YC, Dimonie VL, El-Aasser MS. J Appl Polym Sci 1991;42: 1049–63.

- [23] Winzor CL, Sundberg DC. *Polymer* 1992;33:3797–810.
- [24] Chen YC, Dimonie VL, El-Aasser MS. *Macromolecules* 1991;24:3779–87.
- [25] Karlsson LE, Karlsson OJ, Sundberg DC. *J Appl Polym Sci* 2003;90:905–15.
- [26] Durant YG, Sundberg DC. *Macromolecules* 1996;29:8466–72.
- [27] Stubbs JM, Sundberg DC. *J Coat Technol* 2003;75(938):59–67.
- [28] Kirsch S, Stubbs J, Leuninger J, Pfau A, Sundberg DC. *J Appl Polym Sci* 2004;91:2610–23.
- [29] Hill LW. Dynamic mechanical and tensile properties. In: Koleske JV, editor. *Paint and coating testing manual*. Philadelphia: ASTM; 1995. p. 534–46.
- [30] Ferry JD. *Viscoelastic properties of polymers*. New York: Wiley; 1970 [chapter 10].
- [31] Chu H-H, Lin C-S. *J Polym Res* 2003;10:283–7.
- [32] Doston NA, Galvan R, Laurence RL, Tirrell M. *Polymerization process modeling*. New York: VCH Publishers; 1996 [chapter 7].
- [33] Kroschwitz J, editor. *Kirk-othmer encyclopedia of chemical technology*, vol. 1. Hoboken: Wiley; 2004. p. 342–69.
- [34] Greeley RZ. Free radical copolymerization reactivity ratios. In: Bandrup J, Immergut EH, Grulke EA, editors. *Polymer handbook*. New York: Wiley; 1999. p. II/181–II/337.
- [35] Odian G. *Principles of polymerization*. 3rd ed. New York: Wiley; 1991 [chapter 4]. Zollars RL. *J Appl Polym Sci* 1979;24:1353–70.
- [36] Poehlein GW. *Macromol Symp* 1995;92:179–94.
- [37] Zollars RL. *J Appl Polym Sci* 1979;24:1353–70.
- [38] Fitch RM, Prenosil MB. *J Polym Sci, Part C* 1969;27:95–118.
- [39] Hidalgo M, Cavaille JY, Guillot J, Guyot A, Pichot C, Rios L, et al. *Colloid Polym Sci* 1992;270:1208–21.
- [40] Kim H-B, Wang Y, Winnik MA. *Polymer* 1994;35:1779–86.